IEEE Photonics Journal
An IEEE Photonics Society Publication

Micromachining of Optical Fibers Using Selective Etching Based on Phosphorus Pentoxide Doping

Volume 3, Number 4, August 2011

Simon Pevec
Edvard Cibula
Borut Lenardic
Denis Donlagic

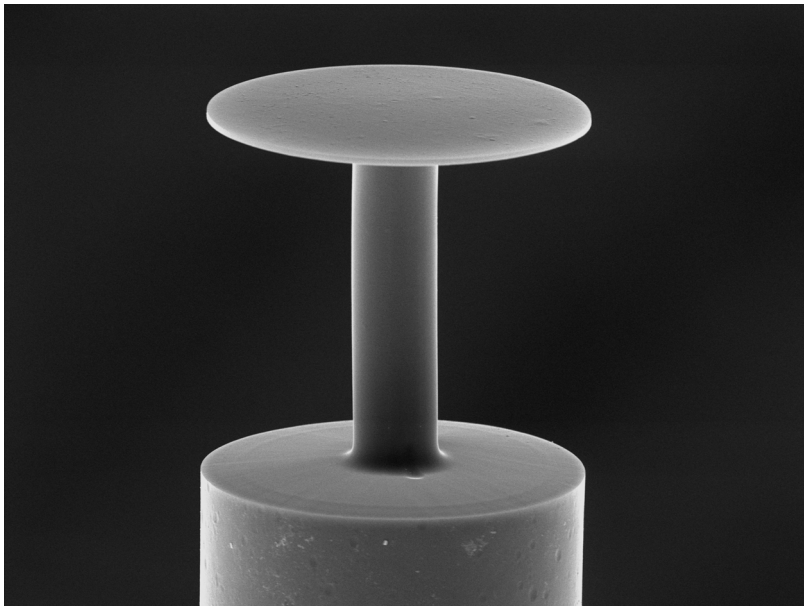

DOI: 10.1109/JPHOT.2011.2159371
1943-0655/$26.00 ©2011 IEEE

IEEE photonics SOCIETY

IEEE

Micromachining of Optical Fibers Using Selective Etching Based on Phosphorus Pentoxide Doping

Simon Pevec,[1] Edvard Cibula,[1] Borut Lenardic,[2] and Denis Donlagic[1]

[1]Faculty of Electrical Engineering and Computer Science, University of Maribor, 2000 Maribor, Slovenia
[2]Optacore d.o.o., 1000 Ljubljana, Slovenia

DOI: 10.1109/JPHOT.2011.2159371
1943-0655/$26.00 ©2011 IEEE

Manuscript received April 23, 2011; accepted June 4, 2011. Date of publication June 13, 2011; date of current version June 28, 2011. This work was supported in part by the Slovenian public research agency under Grant P2-0368. Corresponding author: D. Donlagic (e-mail: ddonlagic@uni-mb.si).

Abstract: This paper presents a maskless micromachining process that can reform or reshape a section of an optical fiber into a complex 3-D photonic microstructure. This proposed micromachining process is based on the etching rate control achieved by the introduction of phosphorus pentoxide into silica glass through standard fiber manufacturing technology. Regions within a fiber cross section doped with phosphorus pentoxide can etch up to 100 times faster than pure silica when exposed to hydrofluoric acid. Various new photonic devices can be effectively and economically created by design and production of purposely doped fibers that are spliced at the tip or in-between standard lead-in fibers, followed by etching into a final structure.

Index Terms: Micro and Nano Opto-Electro-Mechanical Systems (MOEMS), optical fibers, microoptics, advanced optics design.

1. Introduction

Photonic microdevices are being increasingly used in a number of applications, ranging from optical telecommunications [1]–[5] to biomedical sensors [2], [5]–[9]. Direct integration of such devices with optical fibers, can extended their functionality and provide many practical advantages. However, existing micromachining technologies, such as the lithography-based process [10], [11] or direct laser micromachining [12], offer limited possibilities for the direct and economical micromachining of optical fibers. The process for the direct formation of optical devices at the tip, along or within optical fibers, could eliminate these limitations and could enable the creation of a new class of all-fiber microphotonic devices.

It is generally known, that doped silica etches at a different rate than pure silica, when exposed to various etching agents [13]–[15]. In the past, this phenomenon was mostly used as a tool for fiber-refractive index profile analysis [16], [17]. The selective etching achieved by the incorporation of dopants into silica glass can, however, provide a very potent micromachining tool for the formation of complex in-line, in-fiber or at-the-tip fiber-optic devices. For example, when germanium is added to the silica glass, such as in the case of telecom fiber production, the germanium increases the etching rate of the silica [17], [18] in hydrofluoric acid (HF). The change in the etching rate caused by germanium doping is, however, low. In addition, germanium doping causes strong stress buildup in fiber preforms. This restricts the formation of large, preferentially etchable areas within fiber preform cross section and also limits the possibilities for preform mechanical machining that could be otherwise used to create more complex shapes of etchable regions. Fiber micromachining using

germanium doping, therefore, could not extend beyond the formation of simple structures at the fiber's tip, such as cavities for sensor applications [18]–[20], atomic force microscope (AFM) tips [14]–[16], and simple laser-to-fiber coupling [21], [22] devices.

This paper shows that doping with phosphorus pentoxide (P_2O_5) can be used to create high preferentially etchable areas within a fiber cross section, which can be effectively removed upon exposing the fiber to the etching medium. These preferentially etchable P_2O_5-doped areas within the fiber cross section can thus serve as sacrificial layers, which are similar to those in the case of silicon MEMS production, thus allowing for the economical creation of complex all-fiber devices.

2. Impact of Phosphorus Pentoxide Doping on the Etching Characteristic of Silica

The complexities and attributes, such as maximum depth and the achievable aspect ratio of the microstructure, depend on the attainable etching selectivity S of the doped region, which is defined as the ratio between the etching rate of the doped (v_{doped}), and that of the pure silica (v_{SiO_2})

$$S = \frac{v_{\text{doped}}}{v_{SiO_2}}. \tag{1}$$

In order to investigate the impact of P_2O_5 on the etching selectivity S, several differently doped fiber preforms were produced using the modified chemical vapor deposition process (MCVD). Each preform contained between one and five different layers of glass, each doped with a different P_2O_5 concentration. The refractive index profiles of each preform were measured using a preform analyzer. The preforms were then cut into 1 cm-long samples using a low speed diamond saw. The exact radial and axial dimensions of the cut preform samples were measured and recorded. The samples were then etched in 40% HF acid at 25 °C. Depending on the composition of the doped glass, an etching time of between 1 min and 3 h was used to obtain well-defined surface relief. The etching vessel was vibrated to provide acid-mixing and the removal of etching by-products from the sample's surface. The etched-preform samples were then cut in the axial direction through their centers, and were then analyzed/measured under an optical microscope. An example of such an etched preform measurement is shown in Fig. 1. The initial preform diameter and dimensions of the removed doped region were then used to determine the average $v_{\text{doped}}/v_{SiO_2}$ ratio of the individual layers of etched preform. The preform analyzer data and the etching data were then combined to obtain a relationship between the etching selectivity S and the refractive index change caused by doping, which was further correlated to the dopant molar concentration [23]. Several preforms were also drawn into fibers. These fibers were etched and measured under an optical and/or a scanning electron microscope to verify that the fiber drawing did not cause significant change in etching selectivity.

Experimentally measured etching selectivity S, as a function of the concentration of P_2O_5, is shown in Fig. 2, which also shows etching selectivity S for GeO_2-doped silica. These data were added as a reference and were measured in the same way as in the case of the P_2O_5-doped preforms.

As shown in Fig. 2, the P_2O_5 doping of silica can provide very high etching selectivity S, even at low P_2O_5 concentrations. For example, $S = 2.5$ can be achieved at a P_2O_5 concentration corresponding to only 2 mol.%, and $S = 10$ can be achieved at a concentration of approximately 4.8 mol.%. A very high value of $S = 100$ is obtained at around 15.5 mol.% of P_2O_5 (a doping level that is still compatible with most fiber manufacturing processes). Since a low P_2O_5 doping level results in considerable etching selectivity, while inducing only limited fiber preform stress build-up, P_2O_5 doping opens up possibilities for the creation of large and highly preferentially etchable (sacrificial) areas within structure-forming fibers (SFFs). Together with a good compatibility of P_2O_5 with the existing fiber manufacturing process, these properties make phosphorus pentoxide particularly suitable for fiber micromachining purposes.

Several fiber samples drawn from experimental preforms were also etched and measured in baths using different acid concentrations and temperature conditions, in order to determine the

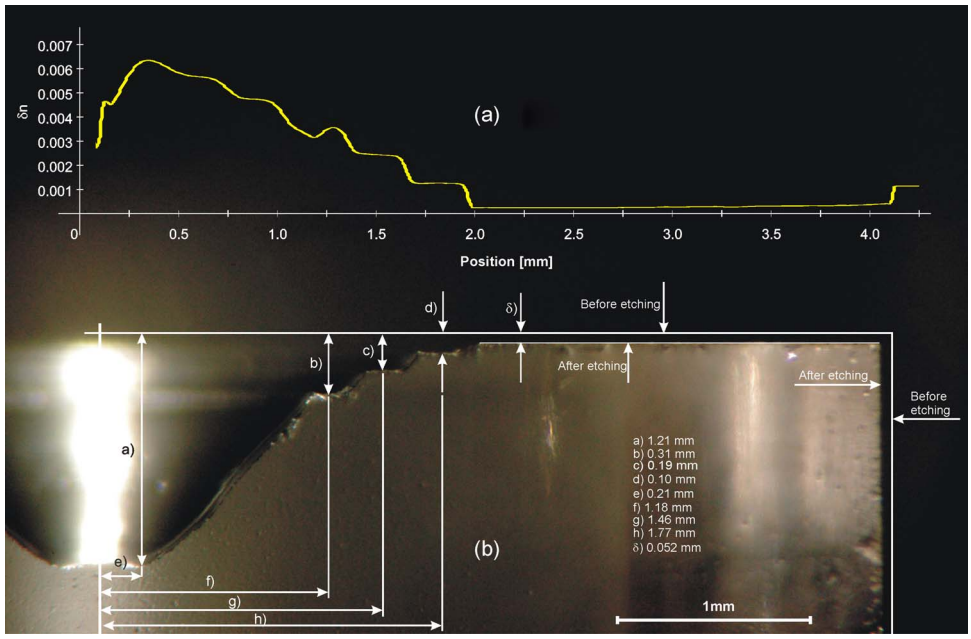

Fig. 1. Typical analysis of etching selectivity on the produced fiber preform. (a) Preform analyzer data. (b) Cross section of the etched perform.

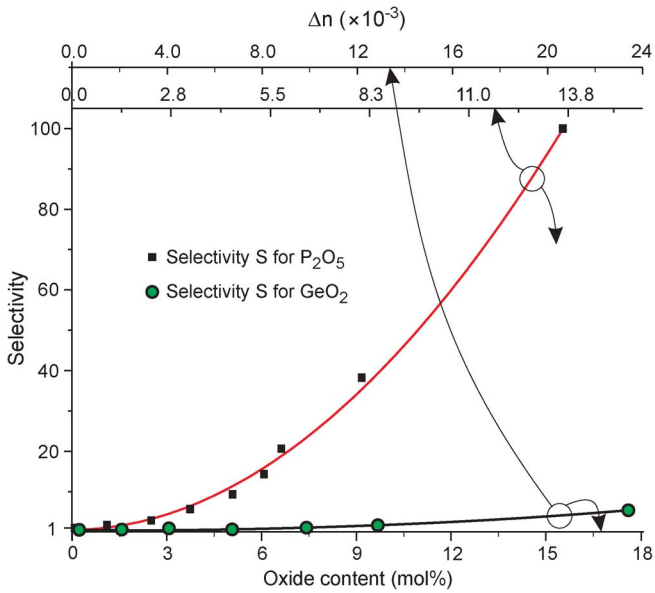

Fig. 2. Etching selectivity S of doped silica in 40% HF at 25 °C as a function of P_2O_5 and GeO_2 concentration.

influences of these parameters on S. Unlike the absolute etching-rate, which exhibits power-law dependence on the temperature, S shows limited dependence on the temperature (see Fig. 3), particularly at lower P_2O_5 concentrations. It is however interesting to observe that etching selectivity depends on acid concentration, particularly at higher P_2O_5 concentrations (e.g., when S is high). A significant drop in etching selectivity can be observed at low HF concentrations. Furthermore, the highest etching selectivity can be achieved by reducing the HF temperature, for example to 0 °C

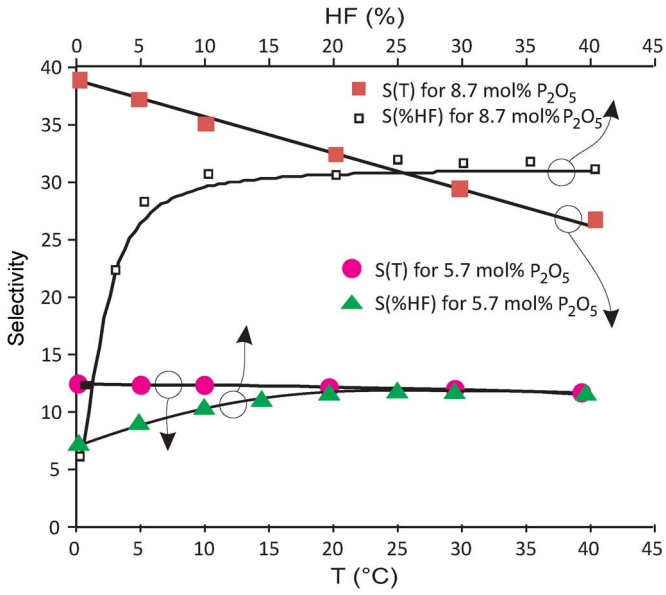

Fig. 3. Temperature and HF concentration impact on *S*.

(this, however, significantly slows down the absolute etching rate and thus increases the time required for the formation of the microstructure).

3. Application of Selective Etching for the Formation of Photonic Microdevices

The possibilities for using selective etching are numerous. In general, the creation of a microdevice based on selective-etching requires the design and manufacturing of a specially doped SFF. A short section of SFF is then spliced at the tip or in-between the lead-in fibers and then etched into the final structure. The tip of the SFF can also be directly etched into the desired microphotonic structure when the SFF incorporates a waveguide structure.

An example of a large and deep cavity formation is demonstrated in Fig. 4. The fiber contained about 75 μm wide, moderately (8.7%mol), P_2O_5-doped region (core). A wide and deep cavity was created upon exposure to HF for a few minutes. The inner-side cavity wall angle corresponded to only 1.6°.

Another, more complex device example produced by selective etching based on P_2O_5 doping is shown in Fig. 4(a), and presents a low-volume all-silica microresonator structure. A cross section of the SFF is shown in Fig. 4(b) and consists of inner pure silica layer, a large P_2O_5-doped-region (5.7%mol), and a thin pure silica outer-layer that has the same glass transition temperature as the lead-in fiber-cladding and, thus, allows for straightforward fusion splicing between them. In order to create this SFF, a standard MCVD technique was used to deposit the P_2O_5-doped cladding and the inner pure silica layer. After characterization, the outer silica layer, consisting of an initial substrate tube, was mechanically removed to a diameter that ensured a proper ratio between the individual preform layers.

The SFF was spliced between two coreless fibers (CFs), with the second CF shortened to a length of about 16 μm, as shown in Fig. 5(c). After the submersion of the spliced-fiber structure into HF, the etchant first uniformly etched the entire structure, but once the pure silica outer-layer of the SFF was removed and HF came into contact with the P_2O_5-doped region, it preferentially removed this region entirely, leaving behind the final structure shown in Fig. 5(a). The total etching time was 12 min in 40% HF at 25 °C. The thickness of the microresonator disk is easily adjustable by adjusting the length of the CF located at the end of the SFF. We successfully made various disks, with thicknesses of above 500 nm (Fig. 5(a) shows a 1.6-μm-thick disk).

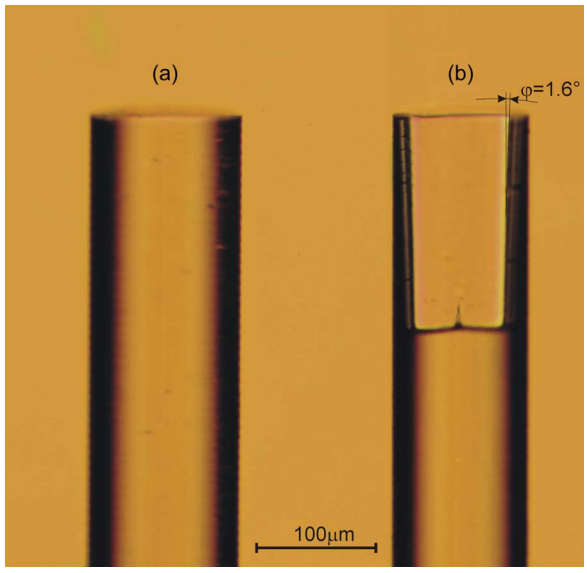

Fig. 4. Wide and deep cavity obtained by P_2O_5 doping. (a) Fiber before etching. (b) The same fiber after 6 min etching in 40% HF.

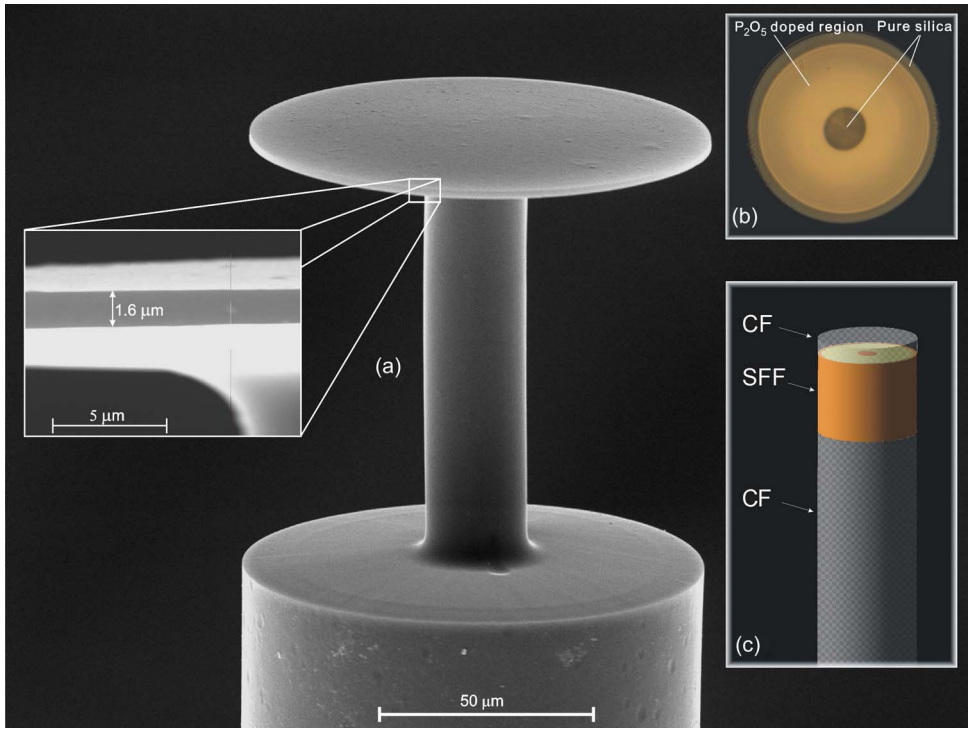

Fig. 5. (a) Scanning electron microscope view of the produced microresonator structure. (b) Optical microscopic cross-sectional view of SFF intended for microresonator structure formation. (c) Fiber

4. Conclusion

This paper investigated optical fiber micromachining process based on selective etching achieved through application of P_2O_5 doping. The results show that P_2O_5 doping can be used to create large highly–preferentially etchable (sacrificial) layers within optical-fibers. This opens up possibilities for

creating complex all-fiber microphotonic devices. In general, the creation of a microdevice based on selective etching requires the design and manufacturing of a specially P_2O_5-doped SFF. While the high etching selectivity obtained by P_2O_5 doping can be utilized in various ways for creating fiber microstructures, typically, a short section of SFF is spliced at the tip or in-between the lead-in fibers and then etched into the target microdevice. The structure's shape control can thus be achieved through the fiber design and manufacturing. Since a single customized SFF production may result in the manufacturing of a large number of devices, the proposed process potentially presents a versatile and efficient way of producing all-fiber devices or device subassemblies.

References

[1] H. Toshiyoshi, "Micro electro mechanical devices for fiber optic telecommunication," *JSME Int. J. Ser. B-Fluids Therm. Eng.*, vol. 47, no. 3, pp. 439–446, 2004.

[2] W. H. Ko, "Trends and frontiers of MEMS," *Sens. Actuators A, Phys.*, vol. 136, no. 1, pp. 62–67, May 2007.

[3] A. Q. Liu and X. M. Zhang, "A review of MEMS external-cavity tunable lasers," *J. Micromech. Microeng.*, vol. 17, no. 1, pp. R1–R13, Jan. 2007.

[4] D. Graham-Rowe, "Fibres get functional," *Nat. Photon.*, vol. 5, no. 2, pp. 66–67, 2011.

[5] T. Takahata, K. Matsumoto, and I. Shimoyama, "A wide wavelength range optical switch using a flexible photonic crystal waveguide and silicon rods," *J. Micromech. Microeng.*, vol. 20, no. 7, p. 075009, Jul. 2010.

[6] R. Bashir, "BioMEMS: State-of-the-art in detection, opportunities and prospects," *Adv. Drug Del. Rev.*, vol. 56, no. 11, pp. 1565–1586, Sep. 2004.

[7] A. C. R. Grayson, R. S. Shawgo, A. M. Johnson, N. T. Flynn, Y. Li, M. J. Cima, and R. Langer, "A BioMEMS review: MEMS technology for physiologically integrated devices," *Proc. IEEE*, vol. 92, no. 1, pp. 6–21, Jan. 2004.

[8] X. D. Hoa, A. G. Kirk, and M. Tabrizian, "Towards integrated and sensitive surface plasmon resonance biosensors: A review of recent progress," *Biosens. Bioelectron.*, vol. 23, no. 2, pp. 151–160, Sep. 2007.

[9] A. Q. Liu, H. J. Huang, L. K. Chin, Y. F. Yu, and X. C. Li, "Label-free detection with micro optical fluidic systems (MOFS): A review," *Anal. Bioanal. Chem.*, vol. 391, no. 7, pp. 2443–2452, Aug. 2008.

[10] B. Culshaw, "Fiber optic sensor—Integration with micromachined devices," *Sens. Actuators A, Phys.*, vol. 47, no. 1–3, pp. 463–469, Mar./Apr. 1995.

[11] C. Liberale, G. Cojoc, P. Candeloro, G. Das, F. Gentile, F. De Angelis, and E. Di Fabrizio, "Micro-optics fabrication on top of optical fibers using two-photon lithography," *IEEE Photon. Technol. Lett.*, vol. 22, no. 7, pp. 474–476, Apr. 2010.

[12] I. B. Sohn, M. S. Lee, J. S. Woo, S. M. Lee, and J. Y. Chung, "Fabrication of photonic devices directly written within glass using a femtosecond laser," *Opt. Express*, vol. 13, no. 11, pp. 4224–4229, May 2005.

[13] Y. Kunii, S. Nakayama, and M. Maeda, "Wet etching of doped and nondoped silicon-oxide films using buffered hydrogen-fluoride solution," *J. Electrochem. Soc.*, vol. 142, no. 10, pp. 3510–3513, Oct. 1995.

[14] S. Mononobe and M. Ohtsu, "Fabrication of a pencil-shaped fiber probe for near-field optics by selective chemical etching," *J. Lightw. Technol.*, vol. 14, no. 10, pp. 2231–2235, Oct. 1996.

[15] F. Dürr, G. Kulik, H. Limberger, R. Salathé, S. Semjonov, and E. Dianov, "Hydrogen loading and UV-irradiation induced etch rate changes in phosphorus-doped fibers," *Opt. Express*, vol. 12, no. 23, pp. 5770–5776, Nov. 2004.

[16] Q. Zhong and D. Inniss, "Characterization of the lightguiding structure of optical fibers by atomic-force microscopy," *J. Lightw. Technol.*, vol. 12, no. 9, pp. 1517–1523, Sep. 1994.

[17] P. Pace, S. T. Huntington, K. Lyytikainen, A. Roberts, and J. D. Love, "Refractive index profiles of Ge-doped optical fibers with nanometer spatial resolution using atomic force microscopy," *Opt. Express*, vol. 12, no. 7, pp. 1452–1457, Apr. 2004.

[18] E. Cibula, D. Donlagic, and C. Stropnik, "Miniature fiber optic pressure sensor for medical applications," in *Proc. IEEE Sens.*, 2002, vol. 1, no. 1, pp. 711–714.

[19] X. P. Chen, F. B. Shen, Z. A. Wang, Z. Y. Huang, and A. B. Wang, "Micro-air-gap based intrinsic Fabry–Perot interferometric fiber-optic sensor," *Appl. Opt.*, vol. 45, no. 30, pp. 7760–7766, Oct. 2006.

[20] E. Cibula, S. Pevec, B. Lenardic, E. Pinet, and D. Donlagic, "Miniature all-glass robust pressure sensor," *Opt. Express*, vol. 17, no. 7, pp. 5098–5106, Mar. 2009.

[21] P. Kayoun, C. Puech, M. Papuchon, and H. J. Arditty, "Improved coupling between laser diode and single-mode fiber tipped with a chemically etched self-centered diffracting element," *Electron. Lett.*, vol. 17, no. 12, pp. 400–402, Jun. 1981.

[22] A. Kotsas, H. Ghafouri-Shiraz, and T. S. M. Maclean, "Microlens fabrication on single-mode fibers for efficient coupling from laser-diodes," *Opt. Quantum Electron.*, vol. 23, no. 3, pp. 367–378, Mar. 1991.

[23] M. M. Bubnov, M. E. Dianov, O. N. Ogorova, S. L. Semjonov, A. N. Guryanov, V. F. Khopin, and E. M. DeLiso, "Fabrication and investigation of single-mode highly phosphorus-doped fibers for Raman lasers," *Proc. SPIE*, vol. 4083, pp. 12–22, 2000.